

An Efficiency-Aware Model Predictive Control Strategy for a Heaving Buoy Wave Energy Converter

Paolino Tona, Hoaï-Nam Nguyen, Guillaume Sabiron, Yann Creff

▶ **To cite this version:**

Paolino Tona, Hoaï-Nam Nguyen, Guillaume Sabiron, Yann Creff. An Efficiency-Aware Model Predictive Control Strategy for a Heaving Buoy Wave Energy Converter. 11th European Wave and Tidal Energy Conference - EWTEC 2015, Sep 2015, Nantes, France. hal-01443855

HAL Id: hal-01443855
https://ifp.hal.science/hal-01443855

Submitted on 23 Jan 2017

HAL is a multi-disciplinary open access archive for the deposit and dissemination of scientific research documents, whether they are published or not. The documents may come from teaching and research institutions in France or abroad, or from public or private research centers.

L'archive ouverte pluridisciplinaire **HAL**, est destinée au dépôt et à la diffusion de documents scientifiques de niveau recherche, publiés ou non, émanant des établissements d'enseignement et de recherche français ou étrangers, des laboratoires publics ou privés.

An Efficiency-Aware Model Predictive Control Strategy for a Heaving Buoy Wave Energy Converter

Paolino Tona, Hoai-Nam Nguyen, Guillaume Sabiron, Yann Creff
IFP Energies nouvelles
IFPEN-Lyon, Rond-point de l'échangeur de Solaize, BP 3, 69360 Solaize, France
E-mail: {name.surname}@ifpen.fr

***Abstract*—In this paper we consider wave energy converters (WECs) of the heaving buoy type. We assume that the available power take-off (PTO) mechanism is able to transform mechanical to electrical power (generator mode) and electrical to mechanical power (motor mode). In this context, a control system can be designed so as to take off as much energy as possible from the waves to the network, for a broad range of sea states. Among the implementable strategies surveyed in the literature, model predictive control (MPC) has the potential to lead to almost optimal performance, because of its ability to deal with many design objectives and performance criteria and to handle constraints on states and control inputs. However, a critical factor is often overlooked in the design and validation of MPC (as well as of most other WEC control strategies): the imperfect power conversion in the PTO. The MPC strategy presented here does take it into account, in the form of a conversion efficiency function in the criterion to be minimised. First, an optimal control problem is formulated and solved offline, which maximises the average net power output of the wave energy converter. Its performance is tested on five scenarios corresponding to different sea states and compared to that of a conventional control, based on proportional–integral (PI) velocity feedback. Then a nonlinear MPC strategy is introduced and its performance is tested on the same scenarios. It is shown that it yields roughly the same results as the optimal control, and can help harvesting up to 50% more energy than the reference PI control.**

***Index Terms*—Wave energy converters, model predictive control, short-term wave prediction, conversion efficiency**

I. Introduction

Among the various Wave Energy Converter (WEC) concepts, many are based on buoyant bodies placed in the sea (see e.g. [1] for a survey). The oscillations caused by the waves passing the body can be converted into electricity by a mechanism called Power Take-Off (PTO). Some PTOs allow four-quadrant operation, i.e. they are able not only to transform mechanical to electrical power (generator mode) but also electrical to mechanical power (motor mode). This feature provides for a great deal of flexibility to control the body motion and bring it into resonance with the incident wave, in order to maximise the net harvested energy.

Among the implementable control strategies that have been proposed in this framework (see [2]), such as proportional velocity feedback control, approximated complex-conjugated control or model predictive control, the latter has the potential to lead to almost optimal performance, because of its ability to deal with many design objectives and performance criteria and to handle constraints on states and control inputs.

Examples of model predictive control (MPC) strategies, based on linear or nonlinear models, convex or non-convex criteria, can be found in [3]–[7]. Most strategies are formulated so as to maximise the net produced energy over a given horizon, which corresponds (for large enough horizons) to the ultimate goal any WEC control system should strive for. However, to the best of our knowledge, no MPC strategy has been proposed so far which takes directly into account the imperfect power conversion in the PTO by introducing a (nonlinear) conversion efficiency, function of the instantaneous power, in the optimisation criterion. Notice that, even though this practice is seldom followed even in the most recent literature, conversion efficiency should be always taken into account in the simulation model to obtain realistic results and a fair comparison among controllers, as shown in [8] for PI velocity feedback control and in [9] for latching control.

Section II describes the system studied, and introduces the mathematical model and control parameterisation used in the following. In Section III, an optimal control problem which takes into account PTO conversion efficiency is formulated and solved offline, assuming complete knowledge of the sea state over the whole optimisation interval. Optimal control results on five different sea states are compared with those obtained with a standard proportional-integral (PI) velocity feedback control strategy, whose parameters are optimised off-line for each sea state. In order to eliminate the need for a far-ahead prediction of the wave force, and overcome the computational burden of the optimal control, a moving-horizon model predictive control (MPC) strategy is introduced in Section IV. Using once again the PI control as a benchmark, it is shown that the MPC strategy can extract up to 50% more power from the waves. The last section gathers the main open issues and future topics worth investigating.

II. System Description

A. Wave Energy Converter Modeling

A wave energy converter of the heaving buoy type, outlined in Fig. 1, is considered. Its mechanics is modelled as a (second order) rotational mass spring damper system. The spring represents the hydrostatic restoring force. The input is

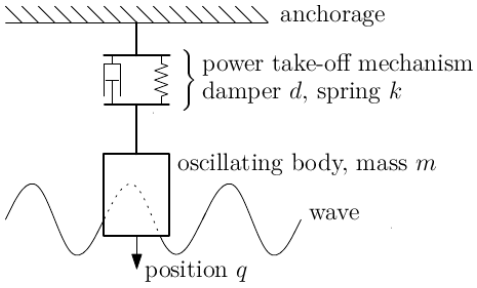


Fig. 1. Simplified model of the considered machine.

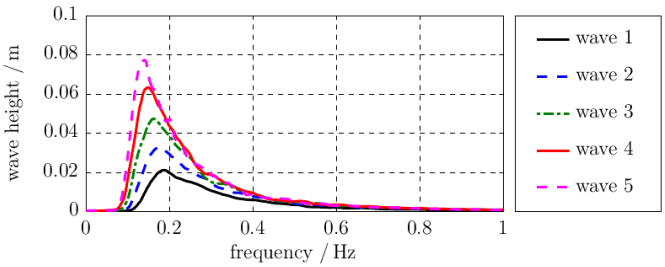


Fig. 3. The (smoothed) spectra of the five considered sea states.

the sum of all acting forces (actuator force, radiation force and wave excitation force) and the output is the velocity. Wave interaction is considered by modelling a radiation resistance force f_r which is calculated from the velocity using order five dynamics. Actuator dynamics is modelled using a second order low-pass filter giving the relationship between the commanded force u_c of the PTO system and the actual force u. The maximum and minimum amplitudes of the force u are limited by physical limitations at $\pm u_{max}$.

A block diagram of the complete model is depicted in Fig. 2. The following system representations are introduced: the actuator dynamics $\boldsymbol{M}_a^c$

$$\dot{\boldsymbol{x}}_a = \boldsymbol{A}_a^c \boldsymbol{x}_a + \boldsymbol{B}_a^c u_c \tag{1}$$
$$u = \boldsymbol{C}_a^c \boldsymbol{x}_a. \tag{2}$$

and the system dynamics $\boldsymbol{M}_s^c$

$$\dot{\boldsymbol{x}}_s = \boldsymbol{A}_s^c \boldsymbol{x}_s + \boldsymbol{B}_s^c (w - u) \tag{3}$$
$$v = \boldsymbol{C}_s^c \boldsymbol{x}_s. \tag{4}$$

which comprises the model of the mechanics and the radiation force. w denotes the wave force which is assumed to be a measurable exogenous signal. In the following, five different realistic sea states with spectra shown (after smoothing) in Fig. 3, are considered for the generation of w.

B. Control Parameterisation and System Discretisation

In the optimal control framework, one often works with parameterised controls. In this work, the standard approach of a piecewise constant control signal is chosen. Accordingly,

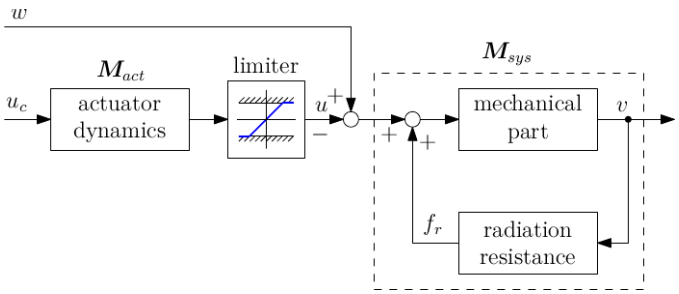


Fig. 2. Structure of the considered mathematical model of the considered machine.

the system dynamics are discretised. The discrete-time counterparts of $\boldsymbol{M}_a^c$ and $\boldsymbol{M}_{sys}^c$ are referred to as $\boldsymbol{M}_a$ and $\boldsymbol{M}_{sys}$. The state-space representation for $\boldsymbol{M}_a$ is

$$\boldsymbol{x}_{a,i+1} = \boldsymbol{A}_a \boldsymbol{x}_{a,i} + \boldsymbol{B}_a u_{c,i} \tag{5}$$
$$u_i = \boldsymbol{C}_a \boldsymbol{x}_{a,i} + \boldsymbol{D}_a u_{c,i}. \tag{6}$$

For the actuator dynamics, a zero-order hold discretisation is chosen in accordance to the piecewise constant parametrisation of the commanded control. Discretised with a zero order hold, the actuator dynamics have no direct feed-through (i. e. $\boldsymbol{D}_a = 0$). But other choices are possible, so a generic $\boldsymbol{D}_a$ is used in the following.

The system dynamics are discretised using Tustin's rule. Both the wave force and the PTO force (the filtered commanded force) are continuous signals s. t. Tustin's rule yields a much better approximation for a given sample time than the zero-order hold. A discretisation using Tustin's rule results in a system representation which is not strictly proper (i. e. $\boldsymbol{D}_s \neq 0$, where $\boldsymbol{D}_s$ is the feed-through matrix for $\boldsymbol{M}_{sys}$).

A sample time of 0.1 sec is selected for the discretisation of both models.

For a certain horizon of n samples, starting to count at sample 0 (i. e. now or $t = 0$), the sampled vectors of commanded/actual control, velocity and wave force are given as

$$\mathfrak{u}_c^T = \left[u_{c,0}, u_{c,1}, \ldots, u_{c,n-1}\right], \tag{7}$$
$$\mathfrak{u}^T = \left[u_0, u_1, \ldots, u_{n-1}\right], \tag{8}$$
$$\mathfrak{v}^T = \left[v_0, v_1, \ldots, v_{n-1}\right], \tag{9}$$
$$\mathfrak{w}^T = \left[w_0, w_1, \ldots, w_{n-1}\right]. \tag{10}$$

Using (5)-(6), the expressions (8)-(10), and the initial values of the actuator and system dynamics, relationships between $\mathfrak{u}$ and $\mathfrak{u}_c$ and between $\mathfrak{v}$ and $(\mathfrak{w} - \mathfrak{u})$ can be established. The actuator dynamics can be written as

$$\mathfrak{u} = \overbrace{\begin{bmatrix} \boldsymbol{D}_a & \boldsymbol{0} & \boldsymbol{0} & \cdots & \boldsymbol{0} \\ \boldsymbol{C}_a\boldsymbol{B}_a & \boldsymbol{D}_a & \boldsymbol{0} & \cdots & \boldsymbol{0} \\ \boldsymbol{C}_a\boldsymbol{A}_a\boldsymbol{B}_a & \boldsymbol{C}_a\boldsymbol{B}_a & \boldsymbol{D}_a & \cdots & \boldsymbol{0} \\ \vdots & \vdots & \vdots & \ddots & \boldsymbol{0} \\ \boldsymbol{C}_a\boldsymbol{A}_a^{n-1}\boldsymbol{B}_a & \boldsymbol{C}_a\boldsymbol{A}_a^{n-2}\boldsymbol{B}_a & \boldsymbol{C}_a\boldsymbol{A}_a^{n-3}\boldsymbol{B}_a & \cdots & \boldsymbol{D}_a \end{bmatrix}}^{\mathfrak{B}_{c\to u}} \mathfrak{u}_c +$$

$$+ \underbrace{\begin{bmatrix} \boldsymbol{C}_a \\ \boldsymbol{C}_a\boldsymbol{A}_a \\ \boldsymbol{C}_a\boldsymbol{A}_a^2 \\ \vdots \\ \boldsymbol{C}_a\boldsymbol{A}_a^n \end{bmatrix}}_{\mathcal{U}_0} \boldsymbol{x}_{a,0} \tag{11}$$

In analogy to $\mathcal{B}_{c\to u}$ and $\mathcal{U}_0$, the matrices $\mathcal{B}_{u\to v}$ and $\mathcal{V}_{0,x}$ are defined for the system dynamics. Using these expressions, the system dynamics can be written as

$$\begin{aligned} \mathcal{v} &= \mathcal{B}_{u\to v}(\mathcal{w} - \mathcal{u}) + \mathcal{V}_{0,x} && (12)\\ &= \mathcal{B}_{u\to v}\left(\mathcal{w} - (\mathcal{B}_{c\to u}\mathcal{u}_c + \mathcal{U}_0)\right) + \mathcal{V}_{0,x}. && (13) \end{aligned}$$

With (11) and (13), the PTO force and the velocity are expressed in terms of the commanded force, the incident wave force and the initial states.

III. Off-line Optimal Control

A. Control Objective

The control objective is to take off the maximum amount of energy/mean power from the considered machine by optimising the PTO control strategy. Since this mean power is taken from the system, it is given a negative sign and thus, the control objective corresponds to the minimisation of the mean power. The mean power P_m^c is easily calculated as the normed integral over the PTO force multiplied with the device velocity and the actuator efficiency η:

$$P_m^c = -\frac{1}{T}\int_{t=0}^{T} \eta u v \mathrm{d}t. \tag{14}$$

In [10], the mean power output is characterised by assuming an almost perfect PTO with losses that are only proportional to the device velocity and $\eta = 1$. In this case, the average mean power that can be taken off the machine can be calculated based on the mean losses, the integral (14) does not need to be evaluated. This characterisation allows for an elegant expression of the mean power output as a convex quadratic function of the control force. It is straightforward to use such an objective function in a standard MPC formulation which can be solved using readily available software tools as done in e. g. [4].

Unfortunately, this formulation of the objective function is unrealistic because the PTO is never one-hundred-percent efficient. This makes power that is taken from the grid more expensive and reduces the value of the generated power. This phenomenon has a great impact on the optimal control and thus cannot be neglected. The phenomenon can be modelled by choosing an efficiency which is a function of the ideal instantaneous power uv:

$$\eta(uv) = \begin{cases} \eta_0 \text{ if } uv \geq 0 \\ \frac{1}{\eta_0} \text{ if } uv < 0 \end{cases}, \; 0 \leq \eta_0 \leq 1 \tag{15}$$

The coefficient η_0 corresponds to the product of the average efficiencies of each PTO stage (actuator, hydraulic transmission if any, generator/motor, inverters). It depends on the PTO and may even differ between the two cases $uv \geq 0$ and $uv < 0$.

Considering (15), the losses depend on the instantaneous power and the elegant formulation from [10] is no longer applicable s. t. it is mandatory to optimise (14) directly.

In order to avoid issues in gradient based optimisation, a smoothed approximation of the function (15), continuous in $uv = 0$, can be used.

B. Formulation of the Optimal Control Problem

In accordance with the previous section, the following optimal control problem has to be solved to harvest the maximum amount of energy from the considered machine:

$$\begin{aligned} &\min_{u_c} P_m^c \text{ s. t.} && (16)\\ &\qquad (1) - (4) \\ &\qquad u_{min} \leq u \leq u_{max} && (17)\\ &\qquad \boldsymbol{x}_{min} \leq \boldsymbol{x} \leq \boldsymbol{x}_{max} && (18) \end{aligned}$$

The mean power P_m^c is a functional of the unknown control signal u_c which can be considered to be an arbitrary function of time. To facilitate the numerical solution of the optimisation problem, the control signal u_c is restricted to being piecewise constant (on an equidistant grid of time) as already mentioned in Section II-B. Instead of the "function" u_c, the sampled vector of the commanded force $\mathcal{u}_c$ is the new vector of decision variables.

C. Reformulation of the Objective Function

Introducing

$$\tilde{\boldsymbol{\eta}}(\mathcal{u}, \mathcal{v}) = \mathrm{diag}\left(\eta(u_0 v_0), \eta(u_1 v_1), \ldots, \eta(u_{n-1} v_{n-1})\right), \tag{19}$$

the integral in the formulation of the instantaneous power P_m^c (15) is reformulated into an Euler integration

$$P_m = -1/T \mathcal{u}^T \tilde{\boldsymbol{\eta}}(\mathcal{u}, \mathcal{v})\mathcal{v}. \tag{20}$$

The optimal control problem can only be solved for a given sea state w (with its sampled counterpart $\mathcal{w}$). It is pointed out explicitly, that the sea state must be known for the complete interval over which the optimal control is to be calculated. The formulation of the velocity vector (13) is rewritten accordingly to highlight the interdependency of velocity and commanded force.

$$\begin{aligned} \mathcal{v} &= \mathcal{B}_{u\to v}\left(\mathcal{w} - (\mathcal{B}_{c\to u}\mathcal{u}_c + \mathcal{U}_0)\right) + \mathcal{V}_{0,x} && (21)\\ &= \underbrace{-\mathcal{B}_{u\to v}\mathcal{B}_{c\to u}}_{\mathcal{B}_{c\to v}}\mathcal{u}_c + \underbrace{\mathcal{B}_{u\to v}\mathcal{w} - \mathcal{B}_{u\to v}\mathcal{U}_0 + \mathcal{V}_{0,x}}_{\mathcal{V}_0} && (22)\\ &= \mathcal{B}_{c\to v}\mathcal{u}_c + \mathcal{V}_0. && (23) \end{aligned}$$

Inserting the discrete-time formulation of the dynamics, i. e.

(11) and (23), into (20), yields

$$P_m = -1/T \left(\mathscr{B}_{c\to u}\mathscr{u}_c + \mathscr{U}_0\right)^T \boldsymbol{\eta}(\mathscr{u}_c) \left(\mathscr{B}_{c\to v}\mathscr{u}_c + \mathscr{V}_0\right) \tag{24}$$

$$\begin{aligned} &= -1/T \mathscr{u}_c^T \mathscr{B}_{c\to u}^T \boldsymbol{\eta}(\mathscr{u}_c) \mathscr{B}_{c\to v} \mathscr{u}_c + \\ &\underbrace{-1/T \left(\mathscr{U}_0^T \boldsymbol{\eta}(\mathscr{u}_c) \mathscr{B}_{c\to v} + \mathscr{V}_0^T \boldsymbol{\eta}(\mathscr{u}_c) \mathscr{B}_{c\to u}\right)}_{\boldsymbol{f}(\mathscr{u}_c)^T} \mathscr{u}_c + \\ &\underbrace{\mathscr{U}_0^T \boldsymbol{\eta}(\mathscr{u}_c) \mathscr{V}_0}_{c_0(\mathscr{u}_c)} \end{aligned} \tag{25}$$

In (25), the function $\tilde{\boldsymbol{\eta}}(\mathscr{u}, \mathscr{v})$ has been replaced with the function $\boldsymbol{\eta}(\mathscr{u}_c)$. The two functions are related as follows

$$\boldsymbol{\eta}(\mathscr{u}_c) = \tilde{\boldsymbol{\eta}}(\mathscr{B}_{c\to u}\mathscr{u}_c + \mathscr{U}_0, \mathscr{B}_{c\to v}\mathscr{u}_c + \mathscr{V}_0). \tag{26}$$

If the efficiency of the PTO $\boldsymbol{\eta}(\mathscr{u}_c)$ is neglected, i. e. if $\boldsymbol{\eta}(\mathscr{u}_c) = 1$, the formulation (25) corresponds to a quadratic cost function. In order to bring it to the standard form

$$1/2 \mathscr{u}_c^T \boldsymbol{H} \mathscr{u}_c + \boldsymbol{f}^T \mathscr{u}_c + c_0, \boldsymbol{H} \text{ symmetric}, \tag{27}$$

the first term in (25) has to be cast into an expression with a symmetric inner matrix $\boldsymbol{H}$. Keeping in mind that P_m is a scalar and using the following property of any scalar s

$$s = (s^T + s)/2, \tag{28}$$

the quadratic term is rewritten as

$$1/2 \mathscr{u}_c^T \overbrace{1/T \left(-\mathscr{B}_{c\to v}^T \boldsymbol{\eta}(\mathscr{u}_c)^T \mathscr{B}_{c\to u} - \mathscr{B}_{c\to u}^T \boldsymbol{\eta}(\mathscr{u}_c) \mathscr{B}_{c\to v}\right)}^{\boldsymbol{H}(\mathscr{u}_c)} \mathscr{u}_c \tag{29}$$

In the simple case $\boldsymbol{\eta}(\mathscr{u}_c) = 1$, the convexity of the objective function can be checked by looking at the definiteness of the inner matrix $\boldsymbol{H}(\mathscr{u}_c)$ in (29). This matrix only depends on the actuator and system dynamics. For the problem data of the considered machine, the objective function is non-convex, because $\boldsymbol{H}(\mathscr{u}_c)$ is not positive semi-definite.

For an efficient solution of the optimal control problem, the gradient of the objective function

$$P_m = 1/2 \mathscr{u}_c^T \boldsymbol{H}(\mathscr{u}_c) \mathscr{u}_c + \boldsymbol{f}(\mathscr{u}_c)^T \mathscr{u}_c + \boldsymbol{c}_0(\mathscr{u}_c) \tag{30}$$

is easily calculated as

$$\begin{aligned} \frac{\partial P_m}{\partial \mathscr{u}_c} = \mathscr{u}_c^T \boldsymbol{H}(\mathscr{u}_c) + 1/2 \mathscr{u}_c^T \frac{\partial \boldsymbol{H}(\mathscr{u}_c)}{\partial \mathscr{u}_c} \mathscr{u}_c + \boldsymbol{f}(\mathscr{u}_c)^T + \\ + \frac{\partial \boldsymbol{f}(\mathscr{u}_c)^T}{\partial \mathscr{u}_c} \mathscr{u}_c + \frac{\partial c_0(\mathscr{u}_c)^T}{\partial \mathscr{u}_c}. \end{aligned} \tag{31}$$

If a non-smooth function for the PTO efficiency is used, the partial derivative in (31) is zero except for the points for which it is not defined. If a smooth approximation of the efficiency $\eta_a(uv)$ is used instead, the partial derivative can be calculated over the whole range of the function.

D. Reformulation of the Constraints

The constraints on the control

$$u_{min} \leq u \leq u_{max} \tag{32}$$

which must hold for all samples of u, i. e. for all entries of $\mathscr{u}$, can be equivalently formulated introducing constraints on the decision variable $\mathscr{u}_c$, through (11). With $\mathbf{1}_{n\times 1}$ denoting an $n \times 1$ matrix of ones, the resulting set of constraints is

$$\mathbf{1}_{n\times 1} u_{min} - \mathscr{U}_0 \leq \mathscr{B}_{c\to u}\mathscr{u}_c \leq \mathbf{1}_{n\times 1} u_{max} - \mathscr{U}_0. \tag{33}$$

The state constraints for the mechanical subsystem can be treated analogously.

E. Smoothing of the Control Signal

In order to avoid unnecessary oscillations in the commanded PTO force u_c, a penalty term for variations of u_c can be added to the control objective. Such a penalty term P_{var} is easily formulated using backward differences. The vector of command variations is

$$\Delta \mathscr{u}_c = \begin{bmatrix} u_{c,0} & u_{c,1} - u_{c,0} & u_{c,2} - u_{c,1} & \dots & u_{c,n-1} - u_{c,n-1} \end{bmatrix}^T \tag{34}$$

$$= \underbrace{\begin{bmatrix} 1 & 0 & 0 & \dots & 0 & 0 \\ -1 & 1 & 0 & \dots & 0 & 0 \\ 0 & -1 & 1 & \ddots & 0 & 0 \\ \vdots & \ddots & \ddots & \ddots & \vdots & \vdots \\ 0 & 0 & 0 & \dots & -1 & 1 \end{bmatrix}}_{\boldsymbol{M}_\Delta} \mathscr{u}_c. \tag{35}$$

Introducing the weight w_{var} which allows to tune the trade-off between desired performance and smoothness of the command, the penalty term P_{var} is chosen as

$$P_{var} = \left(\frac{w_{var}}{u_{max} n} \Delta \mathscr{u}_c\right)^T \left(\frac{w_{var}}{u_{max} n}\right) \Delta \mathscr{u}_c \tag{36}$$

$$= \left(\frac{w_{var}}{u_{max} n}\right) \mathscr{u}_c^T \boldsymbol{M}_\Delta^T \boldsymbol{M}_\Delta \mathscr{u}_c \tag{37}$$

$$= 1/2 \mathscr{u}_c^T \boldsymbol{H}_{var} \mathscr{u}_c \tag{38}$$

The normalisation with $u_{max} n$ helps to choose the weight w_{var}. In essence, if the command jumps from its maximum to its minimum value from sample to sample, a weight $w_{var} = 1$ would lead to an overall penalty term of 2^2. For the results given in this paper, w_{var} is set to 50. The effect of the smoothing is depicted in Fig. 4. Both versions effectively yield the same power output. However, the smoothed control is much less aggressive and thus to be preferred over the non-smoothed. Furthermore, the solution to the optimisation problem with smoothing converges faster.

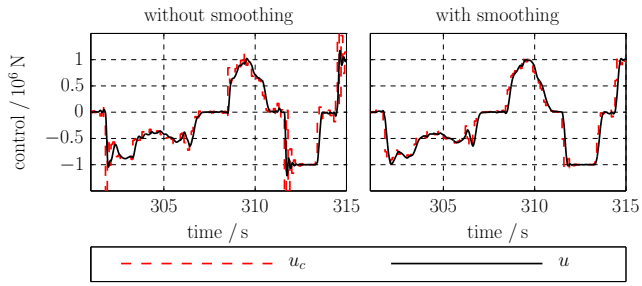


Fig. 4. Impact of the smoothing on the control.

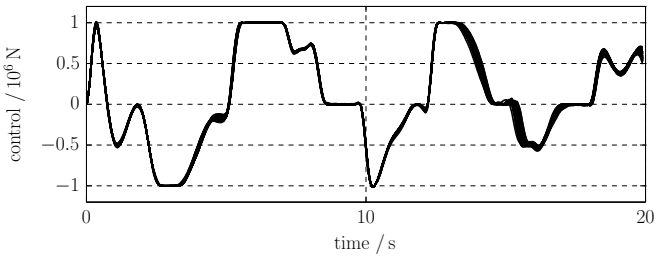


Fig. 5. Optimal control trajectories calculated using random initial values.

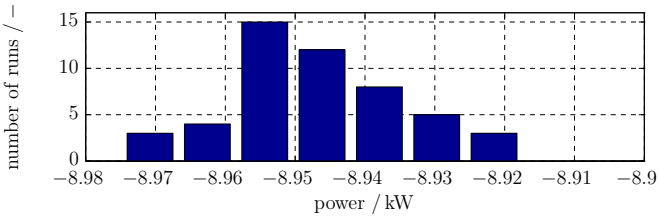


Fig. 6. Distribution of average power harvested with optimal controls calculated using random initial values.

F. Scaling of the Decision Variables and the Objective Function

In order to avoid numerical issues, some scalings are introduced for the decision variables u_c and the objective function. On the one hand, the decision variables are scaled to the bounds of the control signal (u_{max}). On the other hand, the objective function average mean power is scaled to the unit kW which corresponds to an overall scaling factor of $1/1000$.

G. Formulation of the Optimisation Problem

Using the expressions from the previous sections, the overall optimisation problem, which is referred to as the optimal control problem, is

$$\min_{u_c} \; u_c^T \left(\boldsymbol{H}(u_c) + \boldsymbol{H}_{var}\right) u_c + \boldsymbol{f}(u_c)^T u_c + \boldsymbol{c}_0(u_c) \;\text{ s. t.} \tag{39}$$

$$\mathbf{1}_{n\times 1} u_{min} - \mathcal{U}_0 < \mathcal{B}_{c\to u} u_c < \mathbf{1}_{n\times 1} u_{max} - \mathcal{U}_0. \tag{40}$$

The dynamic constraints are implicitly contained in the objective function. State constraints for the mechanical subsystem are not considered to avoid slowing down the computations. If desired, they could be incorporated in analogy to (33).

H. Choice of the Optimisation Algorithm

Since the control objective of (39) is nonlinear and non-convex with a high number of unknowns, a large-scale nonlinear optimisation algorithm is needed. Because the objective function is continuous and an (approximated) gradient can be determined at low computational cost, a gradient-based optimisation algorithm is favoured. Among the freely available solvers available for Matlab falling into the desired category, the interior point algorithm IPOPT [11], interfaced via the OPTI toolbox [12], was chosen, for its performance.

I. Consistency Check of the Optimal Solution

Two different scenarios are considered in order to verify the solution found with IPOPT, i. e. whether a global or a local solution is found, and in order to quantify the possible performance loss.

1) Random Initial Guesses for the Decision Variables: In the first scenario, the same optimal control problem is solved for different random initial choices of u_c. Results from optimisation runs with 50 random initial values for u_c are depicted in Fig. 5. It is clear that the optimisation problem converges toward the same solution for all considered random initial values.

At the same time, the corresponding objective values that are obtained are extremely close as shown in Fig. 6. All results are within a band of about $0.5\,\%$ of the same objective value.

2) Test of the Optimum Principle: The second scenario corresponds to a verification of Bellman's optimum principle. It states that an optimal trajectory has the property that at an intermediate point, no matter how it was reached, the rest of the trajectory must coincide with an optimal trajectory as computed from this intermediate point as the initial, see [13].

In this scenario, two problems are solved. The second problem corresponds to a subproblem of the first, and the optimal control is calculated on an interval starting at an

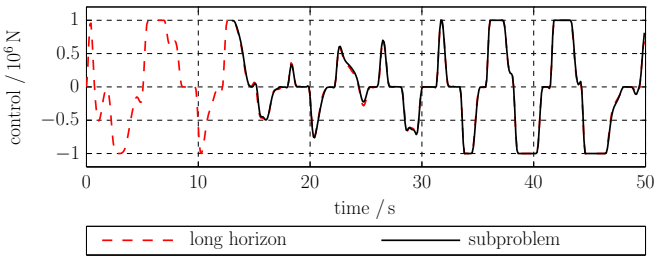


Fig. 7. Verification of the optimum principle: Solution on a sub-interval yields the same trajectory as obtained on the complete interval.

TABLE I
AVERAGE MEAN POWER OUTPUT OF THE OPTIMAL CONTROL WITH DIFFERENT EFFICIENCIES.

	Optimal control				PI
η_0 / -	1	0.9	0.8	0.7	0.7
P_m / kW	-27.86	-22.26	-19.06	-16.32	-12.09

intermediate point from the first problem to the last point of the first problem. Fig. 7 shows that this test is also passed.

J. Application Results and Comparison with Reference Control

The optimal control scenario is solved offline. The execution time of the code is thus unimportant s. t. the problem can be solved over long time horizons. In this case study, a horizon of $n = 2000$ grid points is chosen which corresponds to 200 sec. This section focuses on the optimal control scenario for the sea state 3, i. e. for waves of medium height. The maximum CPU time is set to 15 min. During this time, on a recent but not particularly fast PC (with an Intel i7 CPU at 2.8GHz), the solver can perform about 50 iterations and the solution converges.

As a reference for the performance of the optimal control a standard PI velocity feedback control (also referred to as *BK-control* in [8]) is used:

$$u_c = -k_p \int_{t_0}^{t} v \, \mathrm{d}\tau - k_v v. \tag{41}$$

The proportional gains k_p and k_v are chosen using a gridding approach: for each sea state and time interval considered, the closed loop is simulated for a grid of gains and the combination leading to the best average power output is selected. If well tuned, the PI control law brings the device into resonance with the incident wave.

The optimal control problem is solved for different values of the efficiency $\eta_0 \in \{1, 0.9, 0.8, 0.7\}$ in order to study its impact on the results. For the nominal case $\eta_0 = 0.7$, the obtained optimal trajectory is compared with the results from the PI velocity control, see Fig. 8. In the considered time interval, the optimal control results in higher amplitudes of displacement and velocity.

All results are also gathered in Table I. The average mean power that can be harvested clearly drops significantly if the PTO efficiency is reduced. At the same time, the optimal control avoids to take power from the grid as seen clearly in Fig. 9 (uv is seldom negative). The ratio between the maximum and minimum instantaneous uv is much lower for the high efficiencies.

IV. MOVING HORIZON MODEL PREDICTIVE CONTROL

In order to overcome the computational burden of the optimal control and to eliminate the need for a far-ahead prediction of the wave force, a moving-horizon MPC can be used. The basic idea of moving-horizon MPC is the following:

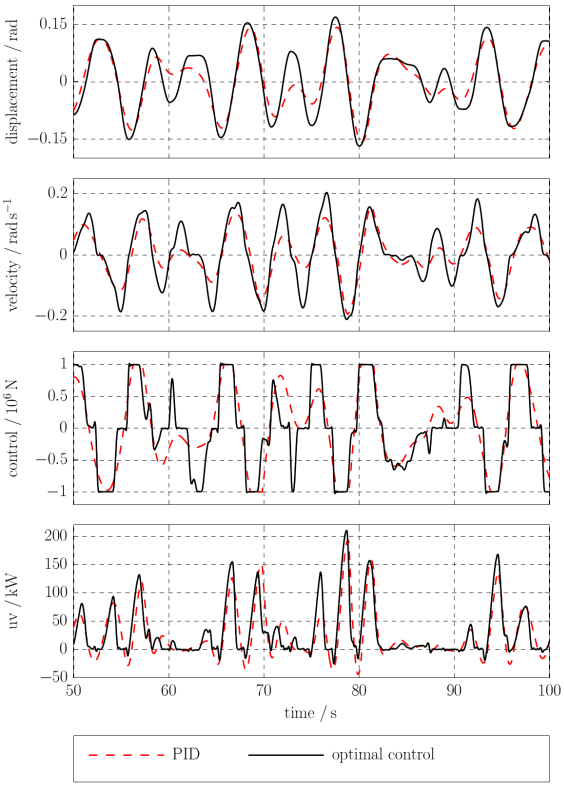


Fig. 8. Comparison of optimal control and PI control for the wave 3.

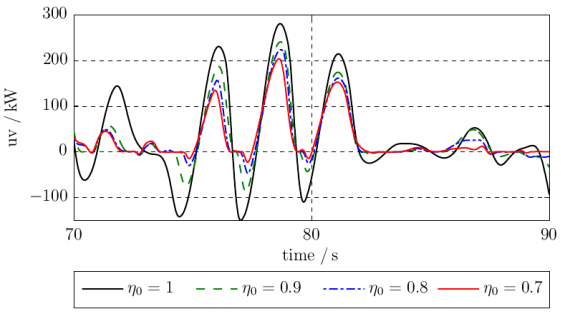


Fig. 9. Instantaneous power with optimal controls for different PTO efficiencies.

1) At current sample i measure (or estimate) the system state and use it as an initial value to calculate an optimal control over a limited horizon with n samples starting at sample i. This yields a time series of optimal control values $u_{c,i}$ of length n.
2) Apply the first value of $u_{c,i}$ (corresponding to the control for the current sample) as a command for the system and hold it for the duration of the sample period.
3) At the next sample $i + 1$, measure the system state and use it again as an initial value to calculate an optimal control over a horizon with n samples starting at $i + 1$. Initialise the vector of decision variables using the results from the previous step. This yields $u_{c,i+1}$

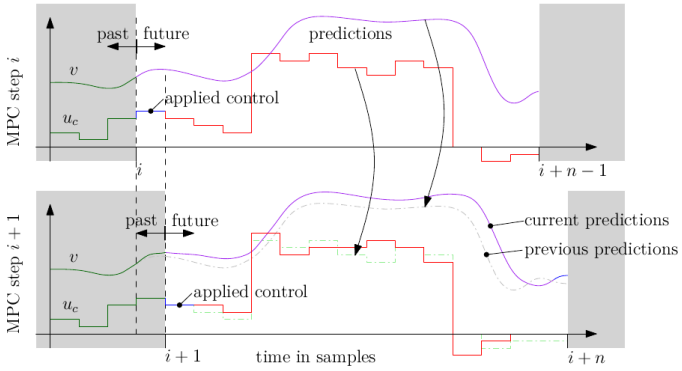


Fig. 10. The principle of sliding horizon MPC.

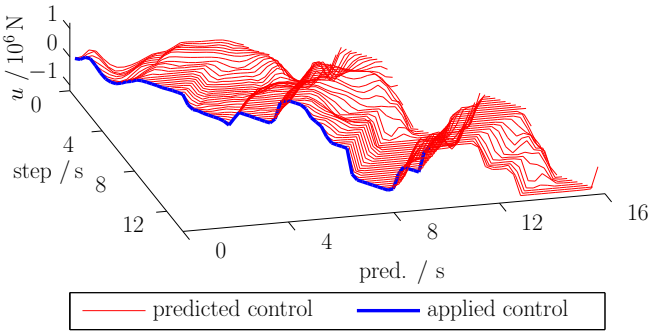


Fig. 11. Applied and predicted controls in a sliding horizon MPC scheme. The red lines represent $u_{c,i}$ in each time step. The first entry, i. e. the applied control, is highlighted in blue.

4) Apply the first value of $u_{c,i+1}$.

$\vdots$

This principle is depicted in Fig. 10.

The main advantages of the moving-horizon MPC scheme is that it is actually implementable in real word applications as an online control law if a short-term wave prediction is available.

A. Penalty for the First Control Value

The transition between the optimal control problem over a single horizon and the moving-horizon problem mainly comes down to the problem of reinitialising the optimisation problem at each time step. To do this correctly, the objective has to be extended in order to penalise the difference between the control for the current step and the previous step $u_{c,pre}$ in analogy to (38)

$$\frac{w_{var}}{u_{max} n} \left(u_{c,0} - u_{c,pre}\right) \left(u_{c,0} - u_{c,pre}\right) \tag{42}$$

$$= \frac{w_{var}}{u_{max} n} \left(u_c^T \begin{bmatrix} 1 & 0 & \dots & 0 \end{bmatrix}^T \begin{bmatrix} 1 & 0 & \dots & 0 \end{bmatrix} u_c - 2 u_{c,pre} \begin{bmatrix} 1 & 0 & \dots & 0 \end{bmatrix} u_c + u_{c,pre}^2 \right). \tag{43}$$

The latter term must be added to the objective function of the optimisation problem (39) which is solved in each step.

B. Compliance with Real-Time Computation Constraints

The prototype control, which is presented in this paper, has not been coded with respect to real-time computation constraints. The control, i. e. the optimisation problem, is solved in a for-loop over the desired time span. In each time step, the optimisation algorithm is terminated after 10 iterations[1] and the first entry of the corresponding $u_{c,i}$ is applied in a continuous time simulation of the model in Simulink. The final values of the simulation are recovered (state feedback) and used to re-initialise the optimisation - all according to the general MPC procedure described in Section IV. Despite this simple implementation, the computational time, including the simulation, is only 2.5 times slower than real-time (on the same not particularly fast PC with a 2.8 GHz processor). Using the profiler option of Matlab, it can be found that only about 45 % of this time is spent solving the MPC problem. Since these results have been obtained without any code optimisation, there is some room to develop a real-time capable version of the control law.

C. Short-Term Wave Prediction

In order to predict the wave force with the methods presented in this section, it must be available as a measurable external signal of the system as assumed in Section II-A (which is quite a strong assumption).

The approach used to predict the waves corresponds to the online identification of an autoregressive (AR) model of the order n_{AR}:

$$y_i = \sum_{k=1}^{n_{AR}} a_k y_{i-k}. \tag{44}$$

The parameter vector

$$\boldsymbol{a} = \begin{bmatrix} a_1 & a_2 & \dots & a_{n_{AR}} \end{bmatrix}^T \tag{45}$$

characterises the AR model.

An equivalent representation of the AR model (44) is found with

$$\begin{bmatrix} y_i \\ y_{i-1} \\ \vdots \\ y_{i-n_{AR}+1} \end{bmatrix} = \begin{bmatrix} a_1 & a_2 & \dots & a_{n_{AR}-1} & a_{n_{AR}} \\ 1 & 0 & \dots & 0 & 0 \\ 0 & 1 & \dots & 0 & 0 \\ 0 & 0 & \ddots & 0 & 0 \\ 0 & 0 & \dots & 1 & 0 \end{bmatrix} \begin{bmatrix} y_{i-1} \\ y_{i-2} \\ \vdots \\ y_{i-n_{AR}} \end{bmatrix}, \tag{46}$$

$$\boldsymbol{x}_i = \boldsymbol{A}_{ar}(\boldsymbol{a}) \boldsymbol{x}_{i-1}, \tag{47}$$

$$y_i = \underbrace{\begin{bmatrix} 1 & 0 & \dots & 0 \end{bmatrix}}_{\boldsymbol{C}_{ar}} \boldsymbol{A}_{ar}(\boldsymbol{a}) \boldsymbol{x}_{i-1}. \tag{48}$$

[1] A termination of the algorithm after only 10 steps is possible because an interior points algorithm is applied which yields a series of feasible points.

Once a suitable model of the type (46) is identified for the wave signal, it may be extrapolated as

$$y_{i+l-1|i-1}(\boldsymbol{a}) = \underbrace{\begin{bmatrix}1 & 0 & \dots & 0\end{bmatrix}}_{\boldsymbol{C}_{ar}} \boldsymbol{A}_{ar}(\boldsymbol{a})^l \boldsymbol{x}_{i-1}. \tag{49}$$

The notation $y_{i+l-1|i-1}(\boldsymbol{a})$ specifies that the l-step-ahead prediction of y is calculated based on measurements up to the step $i-1$ and that this prediction depends on the choice of $\boldsymbol{a}$.

To cover different sea states, the parameter vector $\boldsymbol{a}$ can be optimised online in an iterative way or in a batch job based on recently recorded data. The AR model identification is performed with the objective of minimising a multi-step-prediction over multiple (past) horizons as proposed in [9], [14], [15]. With a finite set of samples $\mathcal{T}$ up to the current one, such a criterion can be formulated as

$$J_{lrp}(\boldsymbol{a}) = \sum_{k\in\mathcal{T}} \sum_{j=1}^{l} \left(y_k - y_{k|k-j}(\boldsymbol{a})\right)^2. \tag{50}$$

Because of (49), this criterion is a nonlinear least squares problem. No constraints on the decision variables $\boldsymbol{a}$ are enforced s. t. the optimisation problem simply reads

$$\min_{\boldsymbol{a}} J_{lrp}(\boldsymbol{a}). \tag{51}$$

It is solved using the adaptive nonlinear least-squares algorithm (NL2SOL) interfaced by the OPTI toolbox. Several options are important to obtain good results for the prediction:

- sample time of the AR model Δt_{AR},
- pre-filtering of the wave signal,
- order of the AR model n_{AR},
- wave prediction horizon (in samples) $n_{w,pred}$.

1) Sample Time of the AR Model: The sample time of the AR model has a huge impact on the prediction quality due to its filtering properties and its impact on the effective prediction horizon $T_{w,pred} = \Delta t_{AR} n_{w,pred}$. It must be chosen according to the dominant wave frequency[2] $f_{w,dom}$.

2) Pre-filtering of the Wave Signal: A pre-filtering of the wave signal can greatly increase the prediction performance, see e. g. [15]. The use of non-causal filtering techniques, to be applied off-line, has been suggested in order to avoid a phase lag of the estimated signal, see [16]. However, since the issues concerning the trade off between non-causality (which can possibly be compensated by a longer prediction horizon) and phase lag have not been solved yet, no pre-filtering of the wave signal is applied in this work.

3) Order of the AR model: The order of the AR model corresponds to twice the number of harmonics that are modelled. There is a trade-off between model complexity (which increases the difficulty to solve the identification problem) and prediction performance. In this work, n_{AR} is set to 32.

[2]The frequency with the highest power.

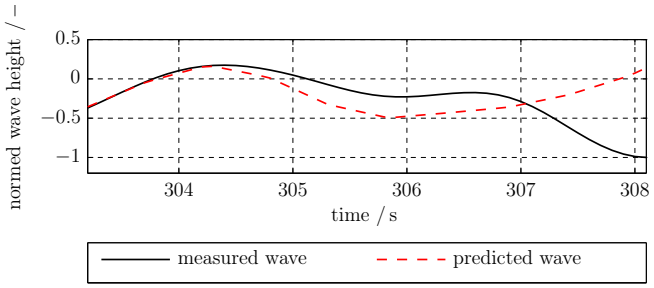


Fig. 12. Wave prediction quality.

4) Prediction Horizon: Like the order of the AR model, this parameter represents a trade-off between the complexity of the identification problem and the prediction performance. A relatively large prediction horizon of $n_{w,pred} = 50$ is chosen. Of that long horizon, only a few first steps approximate the future wave well. The prediction horizon considered in the identification is thus much higher than the prediction horizon needed for the MPC.

Once an AR model is identified, it remains valid for several minutes. In the current implementation, the AR model is updated every 300 sec. Real-time constraints are thus not an issue. The obtained prediction performance for wave 3 is depicted in Fig. 12. It is obvious that it is far from perfect for more than 1 sec into the future. In the final section of this chapter, the performance loss of the MPC control due to an imperfect wave prediction is quantified.

D. State Observation

For the relatively simple linear model considered in this case study, the impact of an imperfect state feedback seems to be negligible. If only the measurable position and velocity are fed back instead of the full state, the performance loss vanishes. The performance loss is established in the subsequent section.

E. Application Results and Comparison with PI Control

The moving-horizon MPC control is applied to the considered machine over the complete time intervals of the available wave data. The nominal case with $\eta_0 = 0.7$ is considered. The results are then compared to the results achieved with PI velocity feedback controllers especially optimised for the respective waves. It should be noted that, in a realistic setting, a gain-scheduling policy has to be implemented in order to adjust the PI gains to the current sea state, which has to be estimated at regular intervals. In contrast to that, the MPC strategy remains the same for all five sea states. Fig. 13, Fig. 14 and Fig. 15 depict the results, i. e. float position and velocity, PTO force and power output of the MPC and the PI control laws, for wave states 1, 3 and 5 respectively. The time intervals correspond to the intervals during which the maximum deflections occur.

A summary of the results is found in Table II. The gain in harvested energy lies between 16 % for high waves and 50 % for low waves.

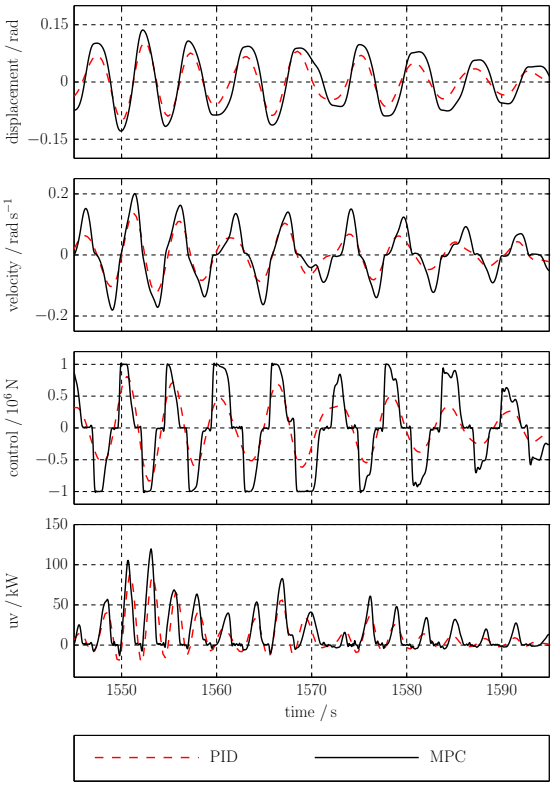


Fig. 13. Comparison of MPC and PI control for the wave 1.

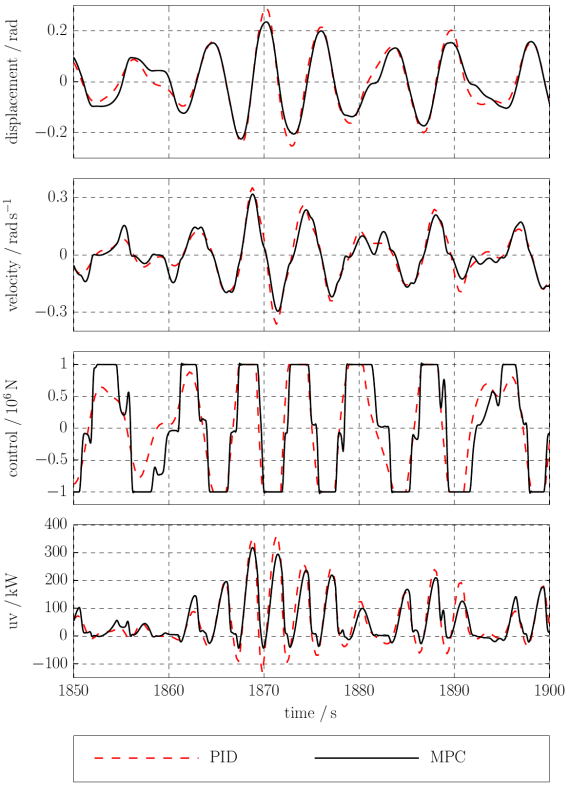


Fig. 14. Comparison of MPC and PI control for the wave 3.

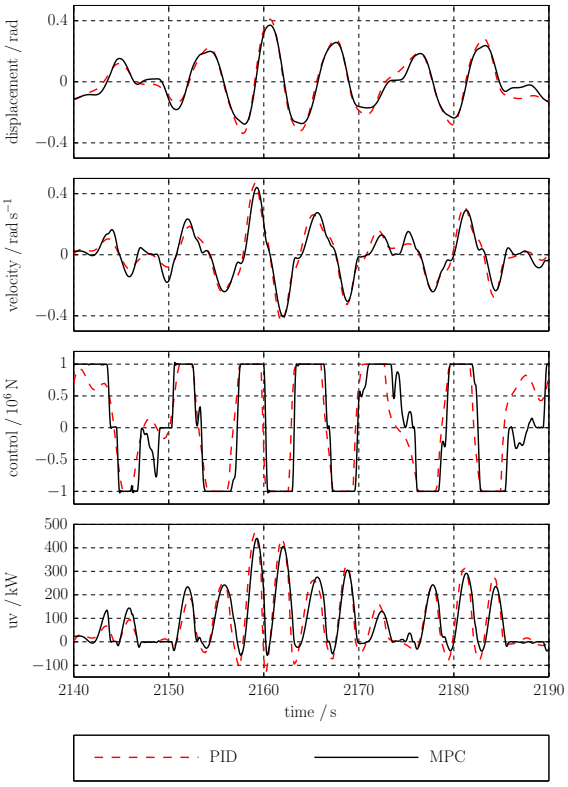


Fig. 15. Comparison of MPC and PI control for the wave 5.

TABLE II
AVERAGE MEAN POWER OUTPUT OF THE MPC CONTROL VS. THE PI CONTROL OVER THE WHOLE TIME INTERVALS OF THE WAVE DATA.

	P_m PI / kW	P_m MPC / kW	gain P_m
wave 1	-2.83	-4.26	50.43 %
wave 2	-8.64	-11.89	37.54 %
wave 3	-16.42	-20.76	26.44 %
wave 4	-24.44	-29.26	19.75 %
wave 5	-32.14	-37.14	15.55 %

For the representative time interval $[301\ \text{sec}, 501\ \text{sec}]$, Fig. 16 depicts the performance gain (with respect to the PI control) of the optimal control, an MPC with state feedback and perfect wave prediction (MPC_1), an MPC with output feedback and perfect wave prediction (MPC_2) and an MPC with output feedback and AR identification based wave prediction (MPC_3).

The perfect MPC and the optimal control practically yield the same results. Most of the performance is lost due to the imperfect wave prediction based on the AR model identification. Compared to the optimal control or perfect MPC, the performance loss with respect to the PI control lies between 3 % and 7 %.

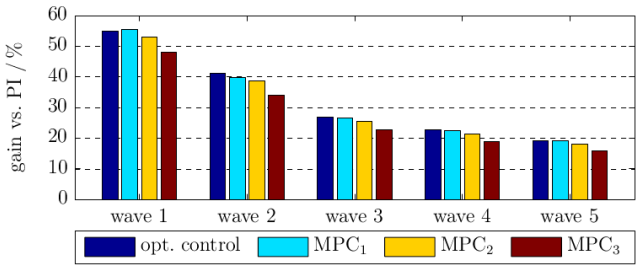


Fig. 16. Performance gain (with respect to the PI control) of the optimal control, an MPC with state feedback and perfect wave prediction (MPC_1), an MPC with output feedback and perfect wave prediction (MPC_2) and an MPC with output feedback and AR identification based wave prediction (MPC_3). Only the representative time interval $[301\ \text{sec}, 501\ \text{sec}]$ is considered.

V. Conclusions

A nonlinear MPC strategy for a wave energy converter of the heaving buoy type has been presented, which takes explicitly into account the conversion efficiency of the PTO system to maximise the mean electrical power extracted from the WEC. It has been shown that the MPC strategy yields results very close to the solution of the corresponding optimal control problem solved offline and has the potential to harvest, depending on the sea state, from 15 to 50% more energy than a conventional controller based on PI velocity feedback.

Nevertheless, a few issues need to be solved and/or further investigated.

A. Short-Term Wave Prediction

The performance of the MPC strategy clearly deteriorates with imperfect wave force prediction. Moreover, the prediction approach adopted here requires periodic analysis of past measurements in order to adapt not only the parameters of the AR model to the current sea state, but also its sample time. Alternative approaches exist, such as in [16], and should be tested in the future to verify if they yield superior performance in combination with the MPC scheme.

B. Availability and Quality of Wave Force Signal

In order to predict future wave force from current and past values, those values must be available. However, wave force is not directly measurable online in a realistic set-up. It can be approximated from wave height measurements, but it must be recalled that a direct measurement of wave height at the center of the float is impossible during normal operation. Some approaches (usually model-based) have already been proposed to estimate it from commonly available sensors, but their performance has yet to be proven for a broad range of operating conditions.

C. Computation Time

Though it seems very likely that, optimising the code, a real-time capable version of the control law should be realisable, the proposed strategy remains intrinsically demanding in terms of computations. To speed up its convergence, it may be advantageous to compute and use an analytic Hessian. Another line of research, which would require some non-obvious theoretical development, consists in trying to convexify the criterion to be minimised.

D. Robustness

The robustness of the design with respect to unmodelled dynamics need to be investigated. It must be established if there are dominant nonlinearities to be considered in the system and how they affect prediction quality and computation time.

VI. Ackowledments

The authors wish to thank Florian Saupe, now consultant at McKinsey & Co., as this paper draws extensively on the research work he did while at IFP Energies nouvelles.

References

[1] B. Drew, A. Plummer, and M. N. Sahinkaya, "A review of wave energy converter technology," *Proceedings of the Institution of Mechanical Engineers, Part A: Journal of Power and Energy*, vol. 223, no. 8, pp. 887–902, 2009. [Online]. Available: http://pep.metapress.com/index/3228075600986163.pdf

[2] J. Hals, J. Falnes, and T. Moan, "A comparison of selected strategies for adaptive control of wave energy converters," *J. Offshore Mech. Arct. Eng.*, vol. 133, no. 3, 2011.

[3] J. Cretel, A. Lewis, G. Lightbody, and G. Thomas, "An application of model predictive control to a wave energy point absorber," in *Control Methodologies and Technology for Energy Efficiency*, vol. 1, no. 1, 2010, pp. 267–272. [Online]. Available: http://www.ifac-papersonline.net/Detailed/43016.html

[4] J. Hals, J. Falnes, and M. Torgeir, "Constrained optimal control of a heaving buoy wave-energy converter," *J. Offshore Mech. Arct. Eng.*, vol. 133 (1), 2010.

[5] T. Brekken, "On model predictive control for a point absorber wave energy converter," in *PowerTech, 2011 IEEE Trondheim*, 2011, pp. 1–8.

[6] M. Soltani, M. Sichani, and M. Mirzaei, "Model predictive control of buoy type wave energy converter," in *Proceedings of 19th IFAC World Congress*. International Federation of Automatic Control (IFAC), 2014.

[7] G. Li and M. R. Belmont, "Model predictive control of sea wave energy converters part i: A convex approach for the case of a single device," *Renewable Energy*, vol. 69, no. 0, pp. 453 – 463, 2014.

[8] E. V. Sanchez, R. H. Hansen, and M. M. Kramer, "Control performance assessment and design of optimal control to harvest ocean energy," *Oceanic Engineering, IEEE Journal of*, vol. 40, no. 1, pp. 15–26, Jan 2015.

[9] F. Saupe, J.-C. Gilloteaux, P. Bozonnet, Y. Creff, and P. Tona, "Latching control strategies for a heaving buoy wave energy generator in a random sea," in *World Congress*, vol. 19, no. 1, 2014, pp. 7710–7716.

[10] J. Falnes, "A review of wave-energy extraction," *Marine Structures*, vol. 20, no. 4, pp. 185–201, 2007. [Online]. Available: http://www.sciencedirect.com/science/article/pii/S0951833907000482

[11] A. Wächter and L. T. Biegler, "On the implementation of an interior-point filter line-search algorithm for large-scale nonlinear programming," *Mathematical Programming*, vol. 106 (1), pp. 25–57, 2006.

[12] J. Currie and D. I. Wilson, "OPTI: Lowering the Barrier Between Open Source Optimizers and the Industrial MATLAB User," in *Foundations of Computer-Aided Process Operations*, N. Sahinidis and J. Pinto, Eds., Savannah, Georgia, USA, 2012.

[13] R. Bellman, "On the Theory of Dynamic Programming," in *Proceedings of the National Academy of Sciences*, vol. 38, 1952, pp. 716–719.

[14] D. Shook, C. Mohtadi, and S. Shah, "Identification for long-range predictive control," *Control Theory and Applications, IEE Proceedings D*, vol. 138, no. 1, pp. 75–84, 1991.

[15] F. Fusco and J. V. Ringwood, "Short-term wave forecasting for real-time control of wave energy converters," *Sustainable Energy, IEEE Transactions on*, vol. 1, no. 2, pp. 99–106, 2010. [Online]. Available: http://ieeexplore.ieee.org/xpls/abs_all.jsp?arnumber=5451110

[16] B. Fischer, P. Kracht, and S. Perez-Becker, "Online-algortihm using adaptive filters for short-term wave prediction and ist implementation," in *Proceedings of the ICOE 2012*, 2012.